Nanoscale

COMMUNICATION

View Article Online
View Journal | View Issue

Cite this: *Nanoscale*, 2016, **8**, 15147

Received 7th June 2016,
Accepted 1st August 2016

DOI: 10.1039/c6nr04615k

www.rsc.org/nanoscale

Self-limiting multiplexed assembly of lipid membranes on large-area graphene sensor arrays†

Michael Hirtz,*‡[a] Antonios Oikonomou,‡[b] Nick Clark,[c] Yong-Jin Kim,[d] Harald Fuchs[a,e] and Aravind Vijayaraghavan*[b,c]

Phospholipid membranes of different functionalities were simultaneously assembled on arrays of graphene surfaces in a parallel manner using multi-pen lipid dip-pen nano-lithography. The graphene patch facilitates and restricts the spreading of lipids within itself, obviating the need to scan the writing probes and reducing writing time. Binding studies establish that the lipids retain the functionality.

Introduction

Graphene has shown tremendous potential in various sensor applications, such as gas-, chemical- and bio-sensors. Generally, pristine graphene is a highly sensitive material, and its various properties such as conductivity, mass, resonance frequency, electron density, *etc*. change significantly upon interaction with the environment, leading to high sensitivity. However, graphene lacks sufficient intrinsic selectivity to able to uniquely identify the nature of the interaction, for example, the molecular species it is sensing. In order to achieve this selectivity, graphene needs to be functionalised with 'receptor' molecules which will specifically recognise and bind with the target analyte.

In attaching receptor molecules to graphene, care should be taken to not affect the intrinsic electronic properties of graphene which are key to its high sensitivity. Generally, non-covalent binding is regarded as superior to covalent binding to preserve graphene's structural and electronic properties. Depending on the nature of the receptor molecule, various approaches have been proposed for non-covalent immobilisation. One approach developed recently is to employ self-assembled bio-mimetic lipid membranes to immobilise biomolecules on graphene. Functionalization of graphene with lipid membranes was first reported by means of vesicles fusion, but drawbacks of this method include the lack of localisation control and inability to multiplex.[1]

One way to achieve ordered and multiplexed lipid membranes in a highly controlled and massively parallel way is by dip-pen nanolithography (DPN)[2] with phospholipids (L-DPN).[3,4] Stacks with single to few layers of smooth lipid membranes can be achieved with this technique.[5] As the resulting membrane stacks exhibit superior properties with regard to minimizing non-specific adhesion of proteins, have high biocompatibility, and can be tuned in function by admixing of functionalized lipids or small molecules as cargo, they found wide application ranging from biological experiments on mast cells,[6,7] drug-delivery experiments,[8] bio-sensing[9] and functionalization of sensor devices.[10–13] Recently, we reported the successful generation of functional biomimetic lipid patches on graphene by L-DPN.[14] Interestingly, we found a high mobility and rapid self-organisation of the lipid membrane on the graphene.

The practical realisation of a graphene-based assay would require multiple functionalities to be assembled in arrays of 10s or 100s micron-sized graphene devices on a single chip. Here we present a way to exploit the spreading of lipids on graphene together with simultaneous L-DPN with a multi-pen array, resulting in a combined top-down and self-assembly approach in the creation of multiplexed graphene supported lipid membrane arrays over large areas.

Results and discussion

Graphene was grown by chemical vapour deposition (CVD) on copper surfaces,[15,16] a self-limiting process which yields monolayer graphene. The graphene was transferred from the copper

[a]*Institute of Nanotechnology (INT) & Karlsruhe Nano Micro Facility (KNMF), Karlsruhe Institute of Technology (KIT), Germany. E-mail: michael.hirtz@kit.edu; Fax: +49 721 608-28976; Tel: +49 721 608-26373*
[b]*National Graphene Institute, The University of Manchester, UK*
[c]*School of Materials, The University of Manchester, UK. E-mail: aravind@manchester.ac.uk; Fax: +44-(0)161-275-4527; Tel: +44-(0)161-275-0136*
[d]*School of Physics and Astronomy, The University of Manchester, UK*
[e]*Physical Institute and Center for Nanotechnology (CeNTech), University of Münster, Germany*

†Electronic supplementary information (ESI) available: AFM image of self-limited spreading on exfoliated graphene, additional fluorescence images. See DOI: 10.1039/c6nr04615k

‡Both authors contributed equally.

on to silicon wafers with 90 nm surface layer of silicon dioxide dielectric using established processes. The graphene was patterned into an array of squares of 20 μm side using optical lithography followed by oxygen plasma etching. For the purposes of this experiment, no electrical contacts were made to the graphene squares, but they essentially represent the graphene sensor arrays that would result after electrical contacts are defined lithographically.

Fig. 1 shows a scheme of the fabrication process for the lipid membrane array. The basic concept is to deliver the desired lipid mixtures to form the graphene supported biomimetic membranes by L-DPN using an array of cantilevers coated in the respective lipid mixtures (Fig. 1a). The deposited lipids spread out to fill the graphene support with a smooth membrane structure (Fig. 1b). Upon immersion into liquid, the membranes reconfigure and the silicon dioxide background is protected against unspecific protein binding by incubation with bovine serum albumin (BSA) that blocks all surface parts not covered by lipid membranes (Fig. 1c). The membrane array can now be incubated with specific proteins that self-assemble onto membrane patches with matching functionality (Fig. 1d).

To elucidate the spreading process, we investigate individual graphene squares by atomic force microscopy (AFM). A single tip was coated with a 1,2-dioleoyl-*sn-glycero*-3-phosphocholine (DOPC) + 5 mol% 1,2-dioleoyl-*sn-glycero*-3-phosphoethanolamine-*N*-(cap biotinyl) (Biotin-PE, both from Avanti Polar Lipids, USA) mixture and then brought into contact with graphene squares for a specified amount of time (dwell time) ranging from 0.1 s to 20 s at a fixed relative humidity of 45%. This allows for different amount of lipid ink to transfer, resulting in initially partial, then complete coverage of the graphene square (Fig. 2). Fig. 2a shows a pristine graphene square, not functionalized by L-DPN. There are some residues remaining from the photolithographic process, especially at the rims of the graphene squares – however, these get engulfed into the membrane upon spreading. Fig. 2b–h shows the increasing coverage of the membrane with increasing dwell time. The lipids spread into well-defined homogeneous membranes, obvious by the flat appearance. When coming into contact with the photoresist residues, the spreading is first slowed down in the respective area in favour to spreading over pristine graphene (see Fig. 2d for a good example), but finally, when overall coverage increases, the membrane simply engulfs also the parts of the graphene covered with residues (Fig. 2f–h). Fig. 2i shows a close up of the membrane area marked in Fig. 2c. An averaged line profile over the black boxed area reveals a membrane thickness of about 4.0 nm, compatible with previous reports on graphene for a single inverted bilayer.[14,17] Even on complete filling of the graphene squares, the lipid membrane remains well contained on the square itself (Fig. 2g and h), spreading stops reliably at the squares border. It should be noted that this seems not to be caused by the photoresist residues occurring at the border of the graphene squares as is evident in the close up presented in Fig. 2j showing the lower left side corner of a completely filled square as marked by a red box in Fig. 2h. Here, the lipid membrane already spread over the resist residues, but still comes to a halt at the graphene square border. Similar self-confinement of lipid-spreading at pristine graphene edges can also be seen on mechanically exfoliated graphene flakes (see ESI Fig. S1†). So the cause for the self-limited spreading must be rather due to the hydrophilicity contrast between the hydrophobic graphene and more hydrophilic silicon oxide background that would require an inversion of the membrane structure for further spreading over this border. Similar containment of lipids based on wetting contrast was also observed for self-assembled monolayers.[17] The authors speculate that graphene might be more hydrophilic than thought (through wetting transparency), but lipid organization on graphene as indicated by thickness measurements in this work and reported in the literature,[14] or by QCM-D[18] indicates that the lipid hydrocarbon chains point towards the pristine graphene, thus indicating hydrophobic nature of the graphene. When comparing the membrane thickness for different coverages (Fig. 2l, showing sections as indicated in Fig. 2e, g and h) that for all dwell times, the spreading results in a single double layer on the graphene. So even though the 10 s dwell time is already sufficient for a complete filling of the square, 20 s dwell time does not give rise to a second level membrane. This indicates that either the transfer of lipid ink stops once a graphene square is completely filled, or perhaps that the areal density of lipids increases to accommodate more molecules on the same area. Fig. 2m plots the area covered by the membrane *vs.* dwell time. In non-limited spreading one would expect a straight line as for a diffusive DPN ink on a border free substrate.[19] This holds true for low coverage (as indicated by a linear fit to the first 4 dwell times, obtaining a transfer constant of 91.8 $\mu m^2\ s^{-1}$), but as the spreading membrane runs out of free graphene area to spread, the speed of spreading declines with the area

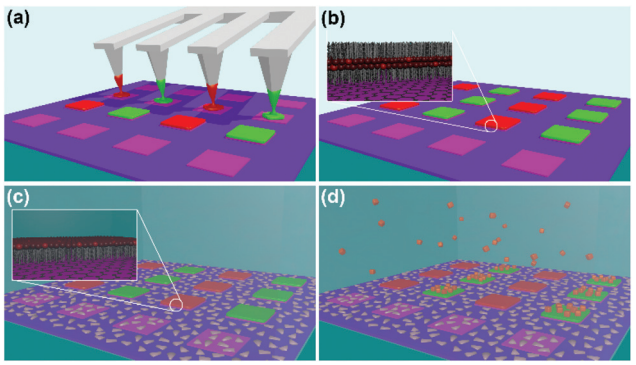

Fig. 1 Scheme of the fabrication process: (a) multiplexed DPN cantilever arrays delivers different lipid mixtures (red and green) to the graphene squares (violet). (b) The lipid mixtures spread to completely fill the graphene squares assembling into double layer membranes. (c) Upon immersion in liquid, the membrane reconfigures into a monolayer. The empty spaces between the graphene squares are passivated by BSA to prevent non-specific protein binding. (d) Proteins can assemble specifically to patches containing matching binding sites.

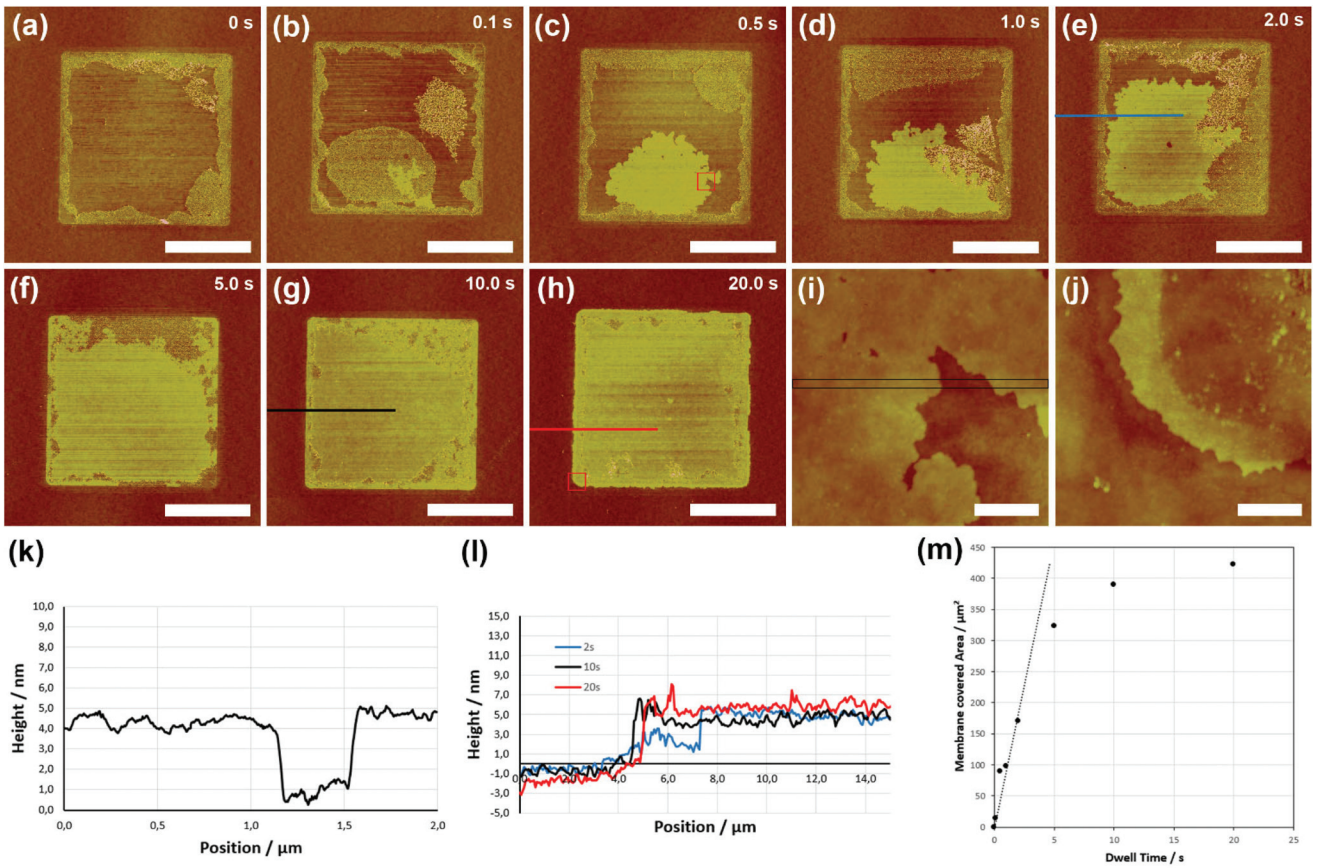

Fig. 2 (a)–(h) AFM images of single squares of graphene (a) before lipid deposition and (b)–(h) after being contacted with a lipid coated tip for 0.1 s, 0.5 s, 1.0 s, 2.0 s, 5.0 s, 10.0 s, and 20.0 s, respectively. Scale bars equal 10 µm. (i) Close up of the area in the red box marked in (c). Scale bar equals 500 nm. (j) Close up of the corner of the graphene square filled for 20.0 s, area marked by red box in (h). Scale bar equals 500 nm. (k) Averaged line profile of the area marked in (i). (l) Overlayed line profiles as indicated in (e), (g), and (h), respectively. (m) Area of spread membrane *versus* dwell time.

approaching the maximum of about 400 µm^2 available on one square.

Traditionally, DPN involves rastering the tip over the sample surface to 'write' molecules in a desired geometrical shape over a specific area. In the case of lipids on graphene, the ready spreading and self-containment effect removes the need to scan the probe, which has a number of associated advantages. Firstly, scanning a probe in contact mode could scratch or damage the graphene under certain conditions. Secondly, we observe that the spreading allows for a lot faster sample fabrication than employing the maximum scan-speed that can still form a continuous membrane, resulting in a much faster process (discussed later). Finally, since there is no real need to precisely contact the probe at the centre of the graphene flake, alignment becomes a lot faster and easier, compared to rastering which requires nanoscale precision in starting and directing the scan to cover a specifically defined graphene square or device.

Fig. 3a shows the inked cantilever array consisting of 12 cantilevers in a 100 µm pitch (M-Probe array, from acst, USA) hovering above the graphene squares sample of matching periodicity. The individual tips of the array were inked alternating with DOPC + 5 mol% 1,2-dioleoyl-*sn-glycero*-3-phosphoethanolamine-*N*-(lissamine rhodamine B sulfonyl) (Rho-PE) and DOPC + 5 mol% Biotin-PE (all from Avanti Polar Lipids, USA) by means of a microfluidic inkwell chip (acst, USA). The reservoirs of the inkwell were filled with 1 µl of the respective solutions at 20 mg ml^{-1} DOPC + the respective admixing in chloroform. After the chloroform is evaporated in a desiccator, the tip array is dipped into the inkwell for 3 minutes at 70% r.H. for coating. After excess ink is bled off on a sacrificial area of the sample by bringing the tip array into contact with the surface, the array is aligned with the graphene squares and the spotting process started. The array is brought into contact with the graphene squares with a dwell time of 3 s at 40% r.H., then shifted by 100 µm to spot the next row of squares. By this process, the resulting pattern is alternating columns of graphene squares with Rho-PE and Biotin-PE containing lipid membrane. Since the membrane self-limited spreading yields the final square shape without the need for writing the shape with the tips directly, the process is much faster than it would be if the squares would

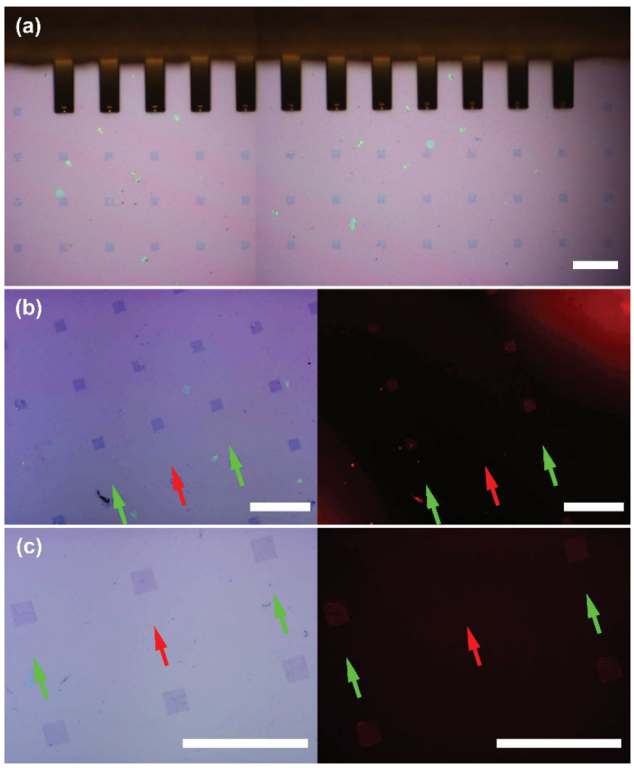

Fig. 3 (a) An array of DPN cantilever alternately inked with Rho-PE/DOPC and Biotin-PE/DOPC lipid mixtures hovering over the graphene square sample during lithography. (b) Optical micrograph (left) and fluorescence micrograph (right) of the graphene squares in liquid after incubation with fluorescently labelled streptavidin. Only the squares that were coated with the Biotin-PE mixture show fluorescence due to the binding of the fluorescent streptavidin. The Rho-PE fluorescence is quenched due to the fluorophore being nearer to the graphene. (c) Close up on six squares. Three corresponding columns are marked in all images to outline the relative positions, red arrow for Rho-PE/DOPC, green arrow for Biotin-PE/DOPC carrying columns, respectively. All scale bars equal 100 μm.

be filled with hatch lines to achieve a square shaped membrane *e.g.* on silicon oxide directly: to pattern 1 × 1 mm^2 of 20 × 20 μm^2 membrane patches with a 100 μm pitch with this technique, it takes only about 0.5 minutes compared to about 30 minutes would the pattern shape be directly written as by typical L-DPN on *e.g.* silicon oxide substrates (assuming 250 nm hatch lines and a line writing speed of 10 μm s^{-1}).

To survey the conformity of the spread membranes and demonstrate retained function, the membrane array was transferred into liquid for protein binding experiments. The sample was first blocked with a 10% BSA solution in phosphate buffered saline (PBS) for 10 minutes to hinder non-specific protein binding on the silicon oxide background, then washed three times by pipetting on and off 50 μl of PBS three times each, and incubated with a streptavidin–cy3 solution (Sigma-Aldrich, Germany) of 1 mg ml^{-1} in PBS for 10 minutes. Before fluorescence images were taken, the sample was washed once more as described above. Fig. 3b and c show representative outcomes of this binding experiment. As it becomes obvious when comparing the bright field images with the corresponding fluorescence microscopy images only the graphene squares with the Biotin-PE containing membranes light up (before streptavidin–cy3 incubation all squares appeared dark in fluorescence), owing to the selective binding of the fluorescently labelled streptavidin to the biotin moieties. While the fluorophore in the Rho-PE containing membrane patches is close to the graphene and therefore fully quenched, the larger distance of the streptavidin–cy3 (by the membrane itself and the proteins size) allows for some residual fluorescence (see also ESI Fig. S2†).

The proposed membrane organization of the graphene supported lipids is shown in Fig. 4. After lithography, which takes place in air, the deposited lipid mixtures spread into homogeneous bilayer membranes (as matching thickness has been observed by AFM). For energetic reasons, it is expected that the hydrophobic hydrocarbon chains are oriented towards the hydrophobic graphene support and also to the air, while the hydrophilic head-groups are buried within the membrane (Fig. 4a). Fluorophores like the Rhodamine in the Rho-PE are coupled to the graphene and get quenched (see ESI Fig. S3†). Upon immersion into liquid the membranes rearrange, now exposing the hydrophilic head-groups to the PBS. Streptavidin present in the solution can bind selectively to the biotin moieties of the Biotin-PE bearing membrane. Since the distance to the graphene is larger, the fluorescence of the streptavidin–Cy3 is not completely quenched. Unspecific binding to the silicon oxide background is prevented by blocking with BSA.

Extrapolating from the 1 × 1 mm^2 written in the described demonstration experiment it becomes feasible to write extremely large areas: *e.g.* writing 1 × 1 cm^2 (containing 100 × 100, *i.e.* 10 000 graphene devices) will still take only 50 minutes (compared to over 2 days on a silicon substrate without benefitting from the self-contained self-assembly). The whole procedure could be sped up even more by further parallelization with 2D arrays (containing up to 55 000 pens) instead of the

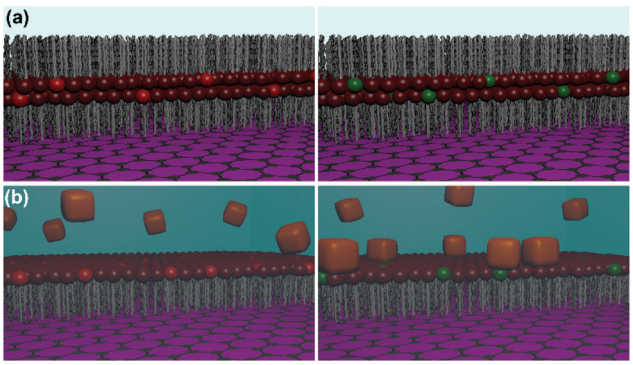

Fig. 4 (a) Scheme of the membrane organization on graphene directly after lithography. DOPC (dark red headgroups) is the main carrier with some admixing of Rho-PE (left, red headgroups) and Biotin-PE (right green headgroups). Membranes are in 'tails out' configuration. (b) Membrane organization on graphene in liquid. Lipid headgroups are exposed to the liquid environment and streptavidin (orange) can bind selectively to the biotin moieties (green, right), while no binding occurs on the Rho-PE containing membranes (left).

1D arrays with only 12 pens.[3,20,21] or the application of stamping-like techniques such as polymer pen lithography (PPL).[22,23] By further exploiting of the multiplexing capability of DPN, which principally allows the application of different lipid mixtures to each individual pen by means of microfluidic networks[24,25] or ink jet methods,[26] or multi-color PPL,[23,27,28] the method will readily be able to rapidly generate well-defined combinatorial lipid membrane arrays of varying composition, *e.g.* for the screening and study of protein lipid interactions.

Conclusions

The self-limited spreading of phospholipids on graphene can be used to generate large area biomimetic membrane arrays in arbitrary shapes on samples pre-structured with graphene. We demonstrate the multiplex capabilities of L-DPN to generate an alternating pattern of lipid membranes with different chemical composition supported by the graphene pre-structures. The process allows a much faster fabrication of large area multiplexed graphene supported membrane arrays than with direct L-DPN writing on silicon oxide or glass. The lipid membranes are stable upon immersion into liquid and specific binding of proteins was shown, opening the route potential application in biological assays and bio-sensing.

Acknowledgements

This work was partly carried out with the support of the Karlsruhe Nano Micro Facility (KNMF, http://www.kit.edu/knmf), a Helmholtz Research Infrastructure at Karlsruhe Institute of Technology (KIT, http://www.kit.edu). AO, NC and AV acknowledge support from EPSRC grants EP/G03737X/1 and EP/G035954/1.

Notes and references

1 P. K. Ang, M. Jaiswal, C. H. Y. X. Lim, Y. Wang, J. Sankaran, A. Li, C. T. Lim, T. Wohland, O. Barbaros and K. P. Loh, *ACS Nano*, 2010, **4**, 7387–7394.
2 R. D. Piner, J. Zhu, F. Xu, S. Hong and C. A. Mirkin, *Science*, 1999, **283**, 661–663.
3 S. Lenhert, P. Sun, Y. Wang, H. Fuchs and C. A. Mirkin, *Small*, 2007, **3**, 71–75.
4 A. Urtizberea and M. Hirtz, *Nanoscale*, 2015, **7**, 15618–15634.
5 M. Hirtz, R. Corso, S. Sekula-Neuner and H. Fuchs, *Langmuir*, 2011, **27**, 11605–11608.
6 S. Sekula-Neuner, J. Maier, E. Oppong, A. C. B. Cato, M. Hirtz and H. Fuchs, *Small*, 2012, **8**, 585–591.
7 E. Oppong, P. N. Hedde, S. Sekula-Neuner, L. Yang, F. Brinkmann, R. M. Dörlich, M. Hirtz, H. Fuchs, G. U. Nienhaus and A. C. B. Cato, *Small*, 2014, **10**, 1991–1998.
8 A. E. Kusi-Appiah, N. Vafai, P. J. Cranfill, M. W. Davidson and S. Lenhert, *Biomaterials*, 2012, **33**, 4187–4194.
9 S. Lenhert, F. Brinkmann, T. Laue, S. Walheim, C. Vannahme, S. Klinkhammer, M. Xu, S. Sekula, T. Mappes, T. Schimmel and H. Fuchs, *Nat. Nanotechnol.*, 2010, **5**, 275–279.
10 U. Bog, T. Laue, T. Grossmann, T. Beck, T. Wienhold, B. Richter, M. Hirtz, H. Fuchs, H. Kalt and T. Mappes, *Lab Chip*, 2013, **13**, 2701–2707.
11 U. Bog, F. Brinkmann, H. Kalt, C. Koos, T. Mappes, M. Hirtz, H. Fuchs and S. Köber, *Small*, 2014, **10**, 3863–3868.
12 P. Rath, M. Hirtz, G. Lewes-Malandrakis, D. Brink, C. Nebel and W. H. P. Pernice, *Adv. Opt. Mater.*, 2015, **3**, 328–335.
13 U. Bog, F. Brinkmann, S. F. Wondimu, T. Wienhold, S. Kraemmer, C. Koos, H. Kalt, M. Hirtz, H. Fuchs, S. Koeber and T. Mappes, *Adv. Sci.*, 2015, **2**, 1500066.
14 M. Hirtz, A. Oikonomou, T. Georgiou, H. Fuchs and A. Vijayaraghavan, *Nat. Commun.*, 2013, **4**, 2591.
15 X. Li, W. Cai, J. An, S. Kim, J. Nah, D. Yang, R. Piner, A. Velamakanni, I. Jung, E. Tutuc, S. K. Banerjee, L. Colombo and R. S. Ruoff, *Science*, 2009, **324**, 1312–1314.
16 S. Bae, H. Kim, Y. Lee, X. Xu, J.-S. Park, Y. Zheng, J. Balakrishnan, T. Lei, H. R. Kim, Y. Il Song, Y.-J. Kim, K. S. Kim, B. Ozyilmaz, J.-H. Ahn, B. H. Hong and S. Iijima, *Nat. Nanotechnol.*, 2010, **5**, 574–578.
17 M. Gavutis, V. Navikas, T. Rakickas, Š. Vaitekonis and R. Valiokas, *J. Micromech. Microeng.*, 2016, **26**, 025016.
18 S. R. Tabaei, W. B. Ng, S.-J. Cho and N.-J. Cho, *ACS Appl. Mater. Interfaces*, 2016, **8**, 11875–11880.
19 B. L. Weeks, A. Noy, A. E. Miller and J. J. De Yoreo, *Phys. Rev. Lett.*, 2002, **88**, 255505.
20 K. Salaita, Y. Wang, J. Fragala, R. A. Vega, C. Liu and C. A. Mirkin, *Angew. Chem., Int. Ed.*, 2006, **45**, 7220–7223.
21 J. Haaheim, V. Val, J. Bussan, S. Rozhok, J.-W. Jang, J. Fragala and M. Nelson, *Scanning*, 2010, **32**, 49–59.
22 F. Huo, Z. Zheng, G. Zheng, L. R. Giam, H. Zhang and C. A. Mirkin, *Science*, 2008, **321**, 1658–1660.
23 F. Brinkmann, M. Hirtz, A. M. Greiner, M. Weschenfelder, B. Waterkotte, M. Bastmeyer and H. Fuchs, *Small*, 2013, **9**, 3266–3275.
24 J.-W. Jang, A. Smetana and P. Stiles, *Scanning*, 2010, **32**, 24–29.
25 S. Sekula, J. Fuchs, S. Weg-Remers, P. Nagel, S. Schuppler, J. Fragala, N. Theilacker, M. Franzreb, C. Wingren, P. Ellmark, C. A. K. Borrebaeck, C. A. Mirkin, H. Fuchs and S. Lenhert, *Small*, 2008, **4**, 1785–1793.
26 Y. Wang, L. R. Giam, M. Park, S. Lenhert, H. Fuchs and C. A. Mirkin, *Small*, 2008, **4**, 1666–1670.
27 Z. Zheng, W. L. Daniel, L. R. Giam, F. Huo, A. J. Senesi, G. Zheng and C. A. Mirkin, *Angew. Chem., Int. Ed.*, 2009, **48**, 7626–7629.
28 G. Arrabito, H. Schroeder, K. Schröder, C. Filips, U. Marggraf, C. Dopp, M. Venkatachalapathy, L. Dehmelt, P. I. H. Bastiaens, A. Neyer and C. M. Niemeyer, *Small*, 2014, **10**, 2870–2876.